Tohoku J. Exp. Med., 2024, **262**, 163-171

Vasohibin-2-Targeting Therapies for the Treatment of Pancreatic Ductal Adenocarcinoma

Yasuhiro Suzuki[1,2] and Yasufumi Sato[1,2]

[1]New Industry Creation Hatchery Center, Tohoku University, Sendai, Miyagi, Japan
[2]Department of Vascular Biology, Institute of Development, Aging, and Cancer, Tohoku University, Sendai, Miyagi, Japan

As pancreatic ductal adenocarcinoma (PDAC) is extremely malignant and refractory, therapeutic options for this cancer are anticipated worldwide. We isolated vasohihibin-2 (VASH2) and observed its overexpression in various types of cancer. We then noticed that upregulated expression of VASH2 in patients with PDAC resulted in a conspicuous reduction in the postoperative survival period and further revealed that the abrogation of *Vash2* expression in pancreatic cancer cells inhibited its growth and metastasis and augmented tumor infiltration of $CD8^+$ cells in the mouse model. We developed VASH2-targeting therapies, 2′,4′-BNA-based antisense oligonucleotide targeting VASH2 (VASH2-ASO) as a nucleotide-based therapy, and VASH2-peptide vaccine as an antibody-based therapy. We also showed that the VASH2-peptide vaccine inhibited PDAC metastasis in an orthotopic mouse model. Here, we expanded our analysis of the efficacy of VASH2-targeting therapies for PDAC. VASH2-ASO treatment inhibited the growth of primary tumors by reducing tumor angiogenesis, normalizing tumor vessels, preventing ascites accumulation and distant metastasis to the liver and lungs, and augmenting the infiltration of $CD8^+$ cells in metastatic tumors. VASH2-peptide vaccine did not affect the infiltration of $CD8^+$ cells into tumors. The present study revealed that VASH2-targeting therapies are promising options for the treatment of PDAC. VASH2-ASO therapy can be administered at any stage of PDAC. Because of the increase of $CD8^+$ cell infiltration, the combination therapy with immune checkpoint inhibitors may be an attractive option. The VASH2-peptide vaccine therapy may be useful for preventing metastasis and/or recurrence after successful initial treatment.

Keywords: modified antisense oligonucleotide; molecular targeting therapy; pancreatic ductal adenocarcinoma; peptide vaccine; vasohibin-2
Tohoku J. Exp. Med., 2024 March, **262** (3), 163-171.
doi: 10.1620/tjem.2023.J109

Introduction

Pancreatic ductal adenocarcinoma (PDAC) is the most malignant refractory cancer. Although surgical resection is the only possible curative treatment, it is often inoperative at an advanced and metastatic stage when diagnosed (Schepis et al. 2023). Moreover, recurrence is common, even after successful surgery (Schepis et al. 2023). Although the incorporation of combined cytotoxic chemotherapy regimens has substantially improved outcomes, the overall 5-year survival rate of PDAC is still less than 10%, and there is an urgent need for the development of effective treatments worldwide (Salazar et al. 2023).

Molecular targeting therapy is a promising option for the treatment of various cancers. Although numerous efforts have been made to establish effective molecular targeted therapies for PDAC, their efficacy is limited (Salazar et al. 2023). Because most PDAC contain mutant *KRAS* (Halbrook et al. 2023), the recent development of KRAS inhibitors has offered considerable hope for the treatment of PDACs. However, the efficacy of KRAS inhibitors in treating PDACs remains unclear (Khan et al. 2023; Gurreri et al. 2023).

We isolated vasohibin-1 (VASH1), which has anti-angiogenic activity, and its homolog vasohibin-2 (VASH2) (Watanabe et al. 2004; Shibuya et al. 2006). It is now evi-

Received November 20, 2023; revised and accepted December 28, 2023; J-STAGE Advance online publication January 12, 2024
Correspondence: Yasufumi Sato, New Industry Creation Hatchery Center, 4-1 Seiryo-machi, Aoba-ku, Sendai, Miyagi 980-8575, Japan. Department of Vascular Biology, Institute of Development, Aging, and Cancer, Tohoku University, 4-1 Seiryo-machi, Aoba-ku, Sendai, Miyagi 980-8575, Japan.
e-mail: yasufumi.sato.b3@tohoku.ac.jp

dent that the *VASH* gene is highly conserved among species. Lower organisms possess a single ancestral *VASH* gene, which has evolved into *VASH1* and *VASH2* genes in vertebrates (Sato 2013). While *VASH1* is preferentially expressed in endothelial cells, *VASH2*, which is closer than *VASH1* to the ancestral *VASH*, is only expressed in the testes after birth (Sato 2013). However, the expression of VASH2 is upregulated in various cancer cells and promotes cancer progression by acting on both cancer cells and cells in the tumor microenvironment (TME), such as endothelial cells (Takahashi et al. 2012; Xue et al. 2013; Kitahara et al. 2014; Suzuki et al. 2017; Norita et al. 2017).

With regard to pancreatic cancer, we have shown that patients with PDAC with high VASH2 expression have a markedly shorter postoperative survival period than patients with low VASH2 expression and have proved that VASH2 is a prognostic factor independent of sex, age, and clinical stage (Kim et al. 2015). We used *LSL-KRas*$^{G12D/+}$, *LSL-Trp53*$^{R172H/+}$, and *Pdx-1-Cre* (*KPC*) mice, a mouse model of PDAC, to demonstrate the involvement of Vash2 in PDAC (Iida-Norita et al. 2019). The knockdown of *Vash2* expression in *KPC* cells did not alter proliferation but significantly reduced invasive and metastatic activities. We then confirmed that the knockout of *Vash2* gene in *KPC* mice significantly reduced peritoneal dissemination and distant metastases of PDACs in a gene-dosage sensitive manner (Iida-Norita et al. 2019). The involvement of VASH2 in pancreatic cancer has been reported by others as well (Tu et al. 2017; Zhang et al. 2018). We therefore regard VASH2 to be an attractive target for the treatment of PDAC.

We have recently developed VASH2-targeting therapies, 2′-*O*,4′-*C*-bridged nucleic acid modified antisense oligonucleotide-targeting VASH2 (VASH2-ASO) as a nucleotide-based therapy (Horie et al. 2023), and VASH2-peptide vaccine as an antibody-based therapy (Lee et al. 2023). We also showed that the VASH2-peptide vaccine was effective in the inhibition of PDAC metastasis in an orthotopic mouse model (Lee et al. 2023). Here, we extended our analysis to the efficacy of VASH2-targeting therapies for PDAC treatment.

Materials and Methods

Murine PDAC cells constitutively expressing firefly luciferase

Murine PDAC cells isolated from *LSL-KRas*$^{G12D/+}$, *LSL-Trp53*$^{R172H/+}$, and *Pdx-1-Cre* (*KPC*) mice with a C57BL/6 genetic background (KPC^{C57} cells) and a derivative clone stably expressing firefly luciferase under the control of a cytomegalovirus promoter (KPC^{C57Luc} cells) have been previously described (Lee et al. 2023). The cells were maintained in Dulbecco's modified Eagle's medium (DMEM) supplemented with 10% fetal bovine serum (FBS).

Gene silencing by VASH2-ASO

KPC^{C57} cells were seeded in six-well plates at 2×10^5 cells/well and cultured overnight in DMEM (FUJIFILM Wako Pure Chemical Corporation, Tokyo, Japan) containing 10% FBS and 1% penicillin/streptomycin (FUJIFILM Wako Pure Chemical Corporation) under 5% CO_2 at 37°C. The following day, the culture medium was replaced with antibiotic-free DMEM containing 10% FBS. The cells were transfected with several different concentrations of VASH2-ASO using Lipofectamine 2000 reagent (Thermo Fisher Scientific, Waltham, MA, USA) according to the manufacturer's protocol. Twenty-four hours after transfection, total RNA was extracted from the cells using the RNeasy Plus Mini Kit (QIAGEN, Hilden, Germany) according to the manufacturer's instructions.

Quantitative real-time reverse transcriptase polymerase chain reaction (qRT-PCR)

To prepare total RNA, KPC^{C57} cells (3×10^5) in six-well tissue culture plates were harvested and total RNA was isolated using an RNeasy mini kit (QIAGEN) according to the manufacturer's instructions. Complementary DNA was prepared from the total RNA using ReverTra Ace (ToYoBo, Osaka, Japan). qRT-PCR was performed using a CFX96 real-time PCR detection system (Bio-Rad, Hercules, CA, USA), according to the manufacturer's instructions. Relative Vash2 mRNA levels were normalized to beta-2-microglobulin (*B2m*) mRNA level. The primer pairs used were as follows: mouse *B2m* forward, 5′-GGTCTTTC TGGTGCTTGTCTCA-3′, and reverse, 5′-GTTCGGC TTCCCATTCTCC-3′; mouse *Vash2* forward, 5′-GGAC ATGCGGATGAAGATCT-3′, and reverse, 5′- CTAGAT CCGGATCTGATAGC-3′.

Western blot analysis

KPC^{C57} cells were incubated with VASH2-AS0 (10 nM) for 24 h and then harvested from the culture dish using a scraper in RIPA buffer containing 0.1% sodium dodecyl sulfate (SDS) (Nakarai, Kyoto, Japan). Protein concentration was calculated using the DC protein assay (Bio-Rad). Equal amounts of proteins were separated via SDS polyacrylamide gel electrophoresis (SDS-PAGE) and blotted onto polyvinylidene fluoride membranes (Bio-Rad). The membranes were then incubated with anti-detyrosinated tubulin (Abcam, Cambridge, UK) and an appropriate horseradish peroxidase (HRP)-conjugated secondary antibody. The bands were detected using the Immobilon Western Chemiluminescent HRP substrate (Merck Millipore, Burlington, MA, USA) and LAS-4000 (Fuji Photo Film, Tokyo, Japan).

Orthotopic mouse model of PDAC

All animal experiments were approved by the Tohoku University Center for Gene Research and were carried out according to the guidelines for animal experimentation of Tohoku University. Wild-type male C57BL/6J mice (8-week-old) were obtained from Charles River Laboratories (Yokohama, Japan).

The orthotopic mouse model of PDAC has been previously described (Lee et al. 2023). Briefly, KPC^{C57Luc} cells

were suspended in ice-cold, serum-free DMEM and gently mixed with an equal volume of ice-cold Matrigel (Corning Life Sciences, Corning, NY, USA). The mice were anesthetized, and a 50 μL of the cell suspension containing 2.5 $\times$ 10^5 KPC^{C57Luc} cells was injected to the pancreatic tail using a 27-gauge-needle. Seven days after implantation, D-luciferin was intraperitoneally injected and tumor engraftment was confirmed via *in vivo* bioluminescence imaging using the IVIS system.

Treatment with 2', 4'-BNA/LNA-based VASH2-ASO

On day 7 after the orthotopic inoculation of KPC^{C57Luc} cells, we started treating the mice. Mice were randomly divided into two groups and administered intraperitoneally with 10 mg/kg of 2′, 4′-BNA/LNA-based VASH2-ASO or its control scramble (Scr) twice a week for 4 weeks, i.e., a total of eight times. On day 34 after the inoculation, mice were euthanized and examined. The primary tumor weight and ascites fluid volume were measured. To evaluate metastasis, the livers and lungs were excised and subjected to *ex vivo* bioluminescence detection using an IVIS system. Bioluminescent signal activity was quantified using Living Image software (Xenogen).

Treatment with VASH2-peptide vaccine

On days 1 and 15 after the orthotopic inoculation of KPC^{C57Luc} cells, the mice were treated with the VASH2-peptide vaccine. Mice were randomly divided into two

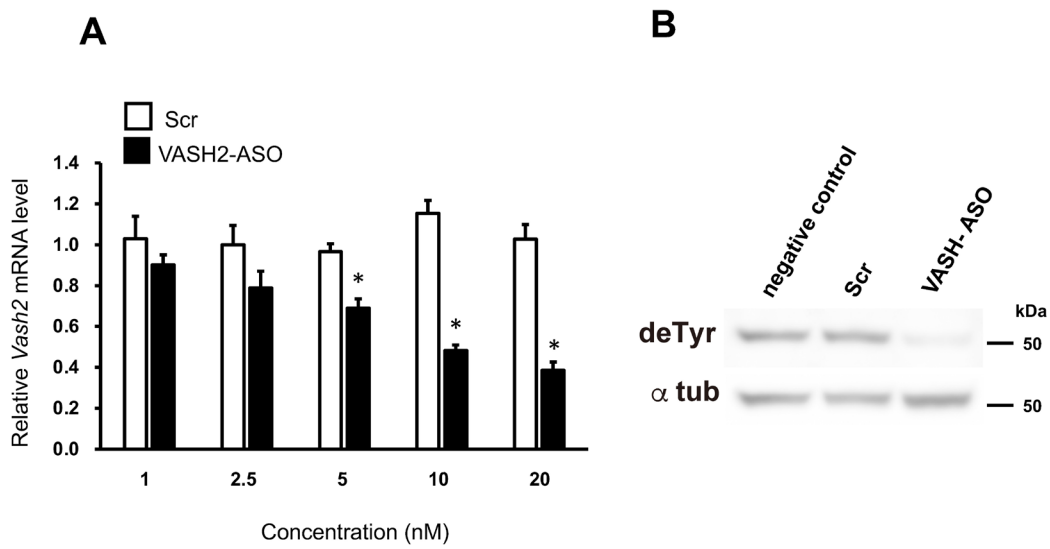

Fig. 1. Effect of VASH2-ASO on the expression of Vash2 in murine pancreatic ductal adenocarcinoma (PDAC) cells in culture. A. KPC^{c57} cells were incubated with the indicated concentrations of VASH2-ASO or control scramble (Scr), and the expression of Vash2 was quantified using qRT-PCR. The expression of Vash2 was inhibited by VASH2-ASO in a dose-dependent manner. Data are presented as the mean ± SD for three independent transfections (n = 3). *$P < 0.05$ by Student's *t*-test. B. KPC^{c57} cells were incubated with 10 nM VASH2-ASO or Scr, and the levels of detyrosinated tubulin (deTyr) and total tubulin were compared via western blotting. VASH2-ASO decreased deTyr levels.

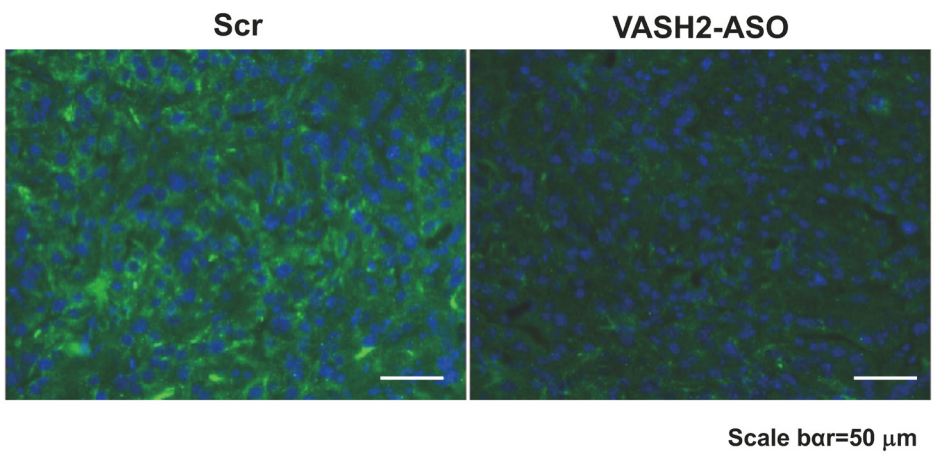

Fig. 2. Effect of VASH2-ASO treatment on the level of detyrosinated tubulin in the primary tumor. Primary tumor tissues were immunostained for detyrosinated tubulin. VASH2-ASO treatment markedly decreased detyrosinated tubulin levels in tumor tissue.

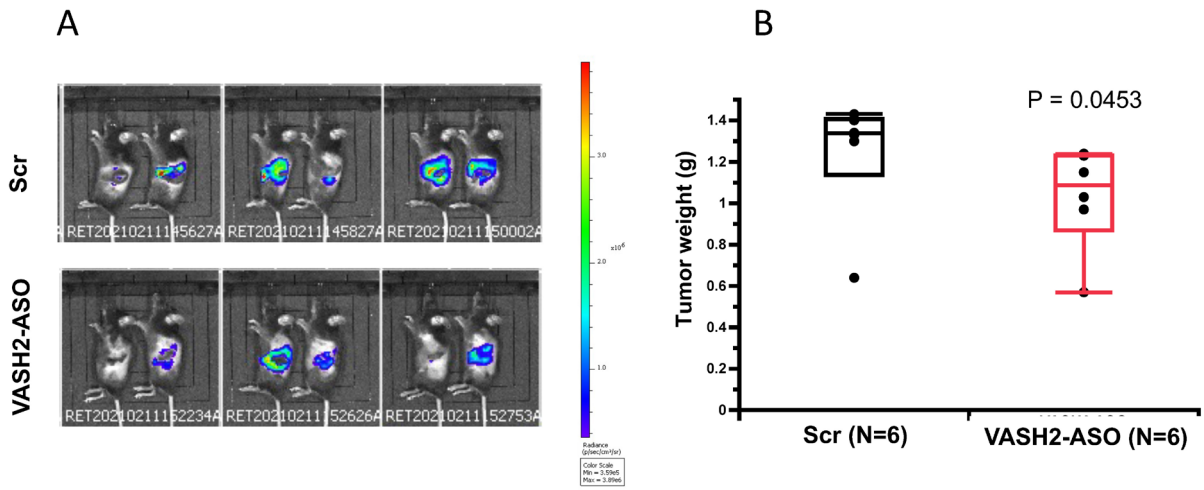

Fig. 3. Effect of VASH2-ASO treatment on the growth of primary tumor.
A. Tumors were visualized with bioluminescence *in vivo* imaging prior to euthanization. B. Primary tumors were obtained and their weights were measured and compared. Quantitative data were presented as box-and-whisker plots. VASH2-ASO treatment significantly inhibited primary tumor growth.

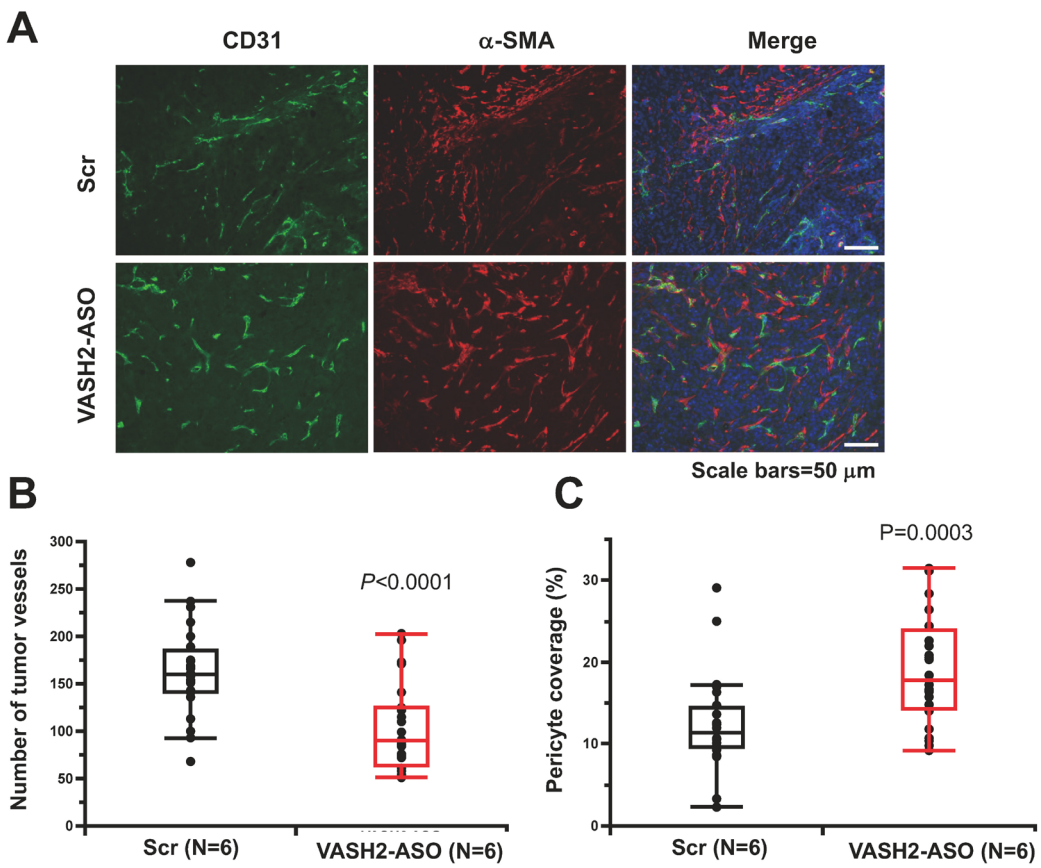

Fig. 4. Effect of VASH2-ASO treatment on tumor angiogenesis.
A. Primary tumors were immunostained for CD31 and α-smooth muscle actin (αSMA). B. The number of tumor vessels in the field was compared. Quantitative data were presented as box-and-whisker plots. C. The percentage of pericyte-covered vessels over the total number of vessels in the field was compared. Quantitative data were presented as box-and-whisker plots. VASH2-ASO treatment significantly inhibited tumor angiogenesis and enhanced vascular maturation.

groups and subcutaneously administered MTG peptide vaccine or control KLH. On day 34 after inoculation, the mice were euthanized and examined. The primary tumor weight and ascites fluid volume were measured. To evaluate metastasis, the livers and lungs were excised and subjected to *ex vivo* bioluminescence detection using an IVIS system. Bioluminescent signal activity was quantified using Living Image software (Xenogen).

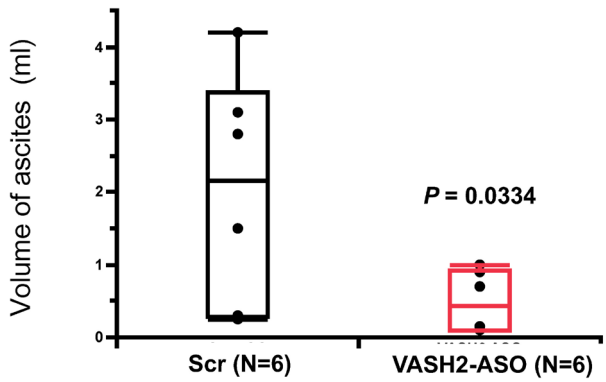

Fig. 5. Effect of VASH2-ASO treatment on ascite acculmation. Accumulated ascitic fluid was obtained, measured, and compared. Quantitative data were presented as box-and-whisker plots. VASH2-ASO treatment significantly inhibited ascitic fluid accumulation.

Immunohistochemical analyses

The primary tumors, liver, and lungs were fixed overnight with 4% paraformaldehyde, dehydrated in graded ethanol and xylene, and embedded in paraffin wax. Tissue sections (5 μm) were prepared for the following immunohistochemical analyses. For immunohistochemical staining, tissue sections were autoclaved in citrate buffer (pH 6.0) for 5 min for antigen retrieval prior to incubation with primary antibodies. Antibodies against detyrosinated α-tubulin (Abcam, Cambridge, MA, USA), CD31, and CD8 (Cell Signaling Technology, Beverly, MA, USA) were used as the primary antibodies. The staining signals were visualized using Histofine Simple Stain MAX PO (Nichirei, Tokyo, Japan), followed by counterstaining with hematoxylin. For fluorescence immunostaining, antibodies conjugated with Alexa Fluor 488 (Thermo Fisher Scientific) were used as the secondary antibodies. The nuclei were counterstained with DAPI (Thermo Fisher Scientific). Tissue autofluorescence was eliminated using the TrueVIEW autofluorescence quenching kit (Vector Laboratories, Peterborough, UK). Microphotographs and fluorescent images were captured using a KEYENCE BZ-9000 microscope (Keyence Corporation, Osaka, Japan).

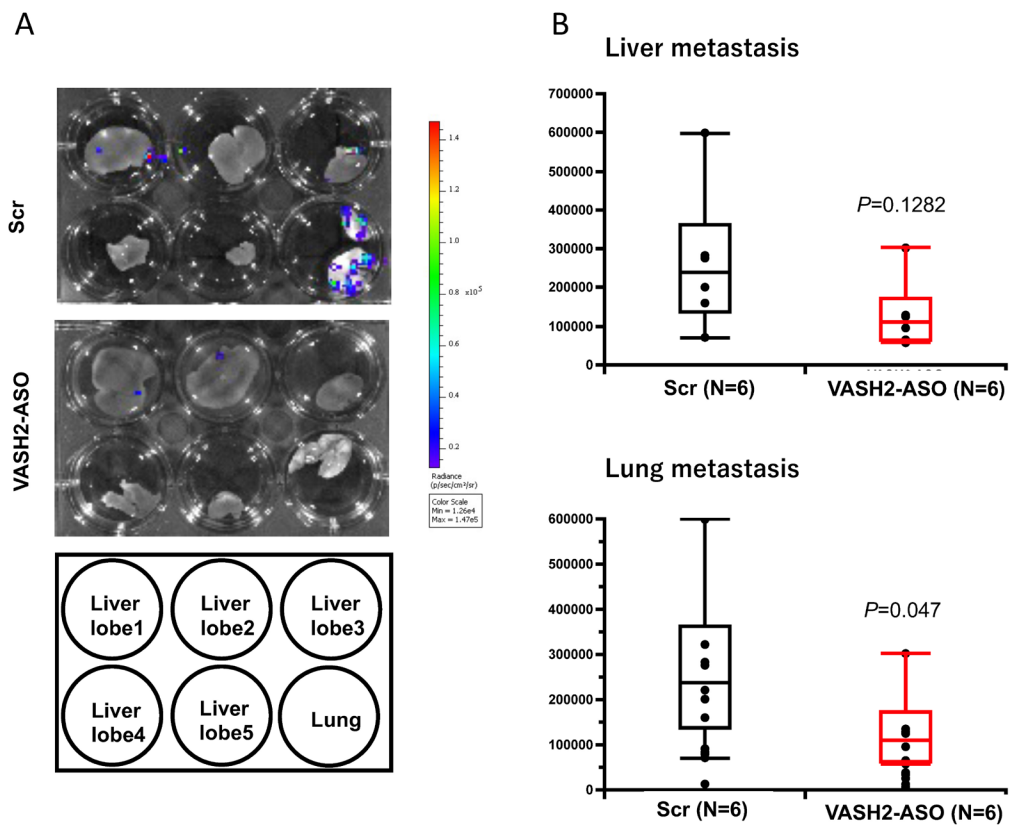

Fig. 6. Effect of VASH2-ASO treatment on distant metastases to the liver and the lungs. The livers and lungs were excised and subjected to *ex vivo* bioluminescence imaging. A. The representative images are shown. B. Bioluminescence is shown. Quantitative data are presented as box-and-whisker plots. VASH2-ASO treatment significantly inhibited distant metastases to the liver and lungs.

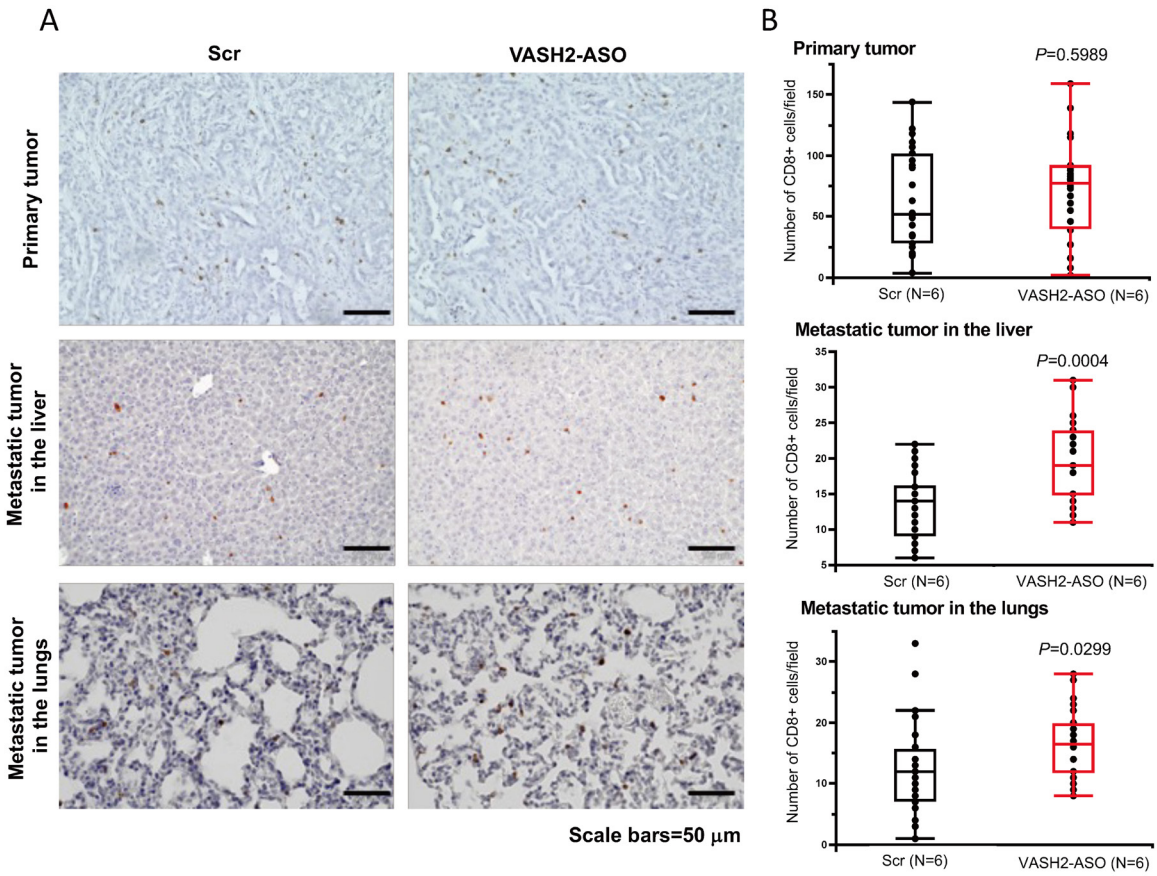

Fig. 7. Effect of VASH2-ASO treatment on the infiltration of CD^{8+} cells in primary and metastatic tumors.
A. Primary tumors, metastatic tumors in the liver, and metastatic tumors in the lungs were immunostained for CD^{8+} cells. B. The numbers of CD^{8+} cells in the field are compared. Quantitative data are presented as box-and-whisker plots. VASH2-ASO treatment significantly increased CD^{8+} cell infiltration in metastatic tumors.

Statistical analysis

Student's *t*-test or Wilcoxon rank-sum test was used to test for significant differences. Statistical significance was set at $P < 0.05$.

Results

We have previously designed and selected the best nucleotide sequence of VASH2-ASO to target human *VASH2* gene, which is located in exon 7 (Horie et al. 2023). The same nucleotide sequence was present in exon 6 of the murine *Vash2* gene, which is common to the two splicing variants of murine *Vahs2* mRNA (Supplementary Fig. S1). Therefore, we considered that our VASH2-ASO should also function in murine systems. To test this hypothesis, murine PDAC cells (KPC^{c57}) were cultured with VASH2-ASO. As shown in Fig. 1A, VASH2-ASO inhibited the expression of *Vahs2* mRNA in a dose-dependent manner. As VASH2 possesses tubulin carboxypeptidase (TCP) activity (Aillaud et al. 2017; Nieuwenhuis et al. 2017), we examined the detyrosination of α-tubulin and confirmed the knockdown effect of VASH2-ASO (Fig. 1B). Based on these results, we proceeded to conduct a therapeutic experiment of PDAC in an orthotopic mouse model.

We repeated intraperitoneal injections of naked VASH2-ASO 8 times at an interval of 3-4 days and tested the therapeutic efficacy in the orthotopic mouse model of PDAC. First, we evaluated primary tumors. Immunohistochemical analyses of detyrosinated α-tubulin showed that the intraperitoneal injection of VASH2-ASO exerted the knockdown effect in the primary tumor (Fig. 2). Primary tumor growth was slightly but significantly inhibited by VASH2-ASO treatment (Fig. 3). We immunohistochemically examined the tumor vessels (Fig. 4A) and found that tumor angiogenesis was inhibited in parallel with tumor growth (Fig. 4B). In addition, more pericytes covered the tumor vessels, indicating vascular maturation (Fig. 4C).

We examined the invasion and metastasis of PDAC cells. Ascites is a sign of peritoneal dissemination, and VASH2-ASO treatment significantly inhibited the accumulation of ascites (Fig. 5). VASH2-ASO treatment also inhibited the distant metastasis of PDAC to the liver and lungs (Fig. 6), although the difference was not significant in liver metastasis.

We then examined the infiltration of $CD8^{+}$ cells into the tumors. Immunohistochemical analyses revealed that VASH2-ASO treatment significantly increased $CD8^{+}$ cell

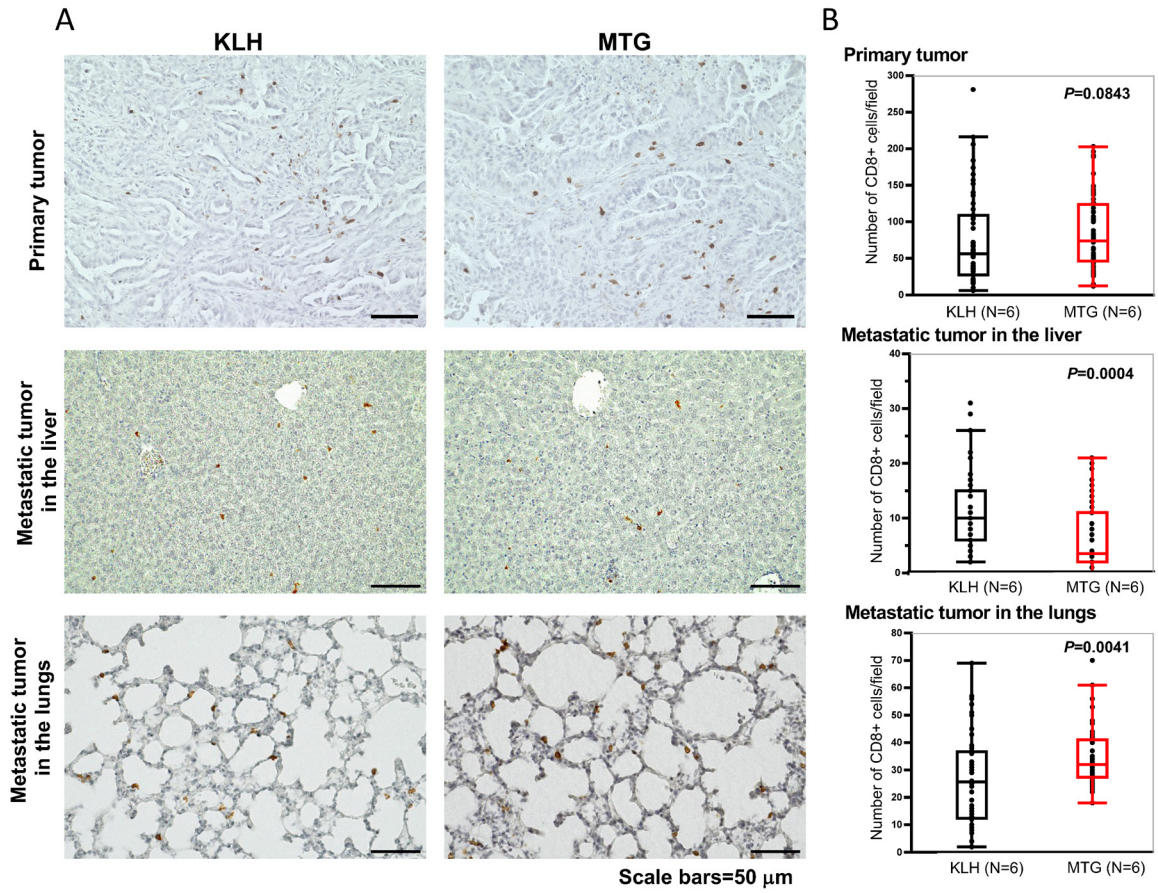

Fig. 8. Effect of VASH2-peptide vaccine treatment on the infiltration of CD^{8+} cells in primary and metastatic tumors. A. Primary tumors, metastatic tumors in the liver, and metastatic tumors in the lungs were immunostained for CD^{8+} cells. B. The numbers of CD^{8+} cells in the field are compared. Quantitative data are presented as box-and-whisker plots. The VASH2-peptide vaccine treatment did not affect the infiltration of CD^{8+} cells.

infiltration, especially in the metastatic tumors of the liver and lungs (Fig. 7).

We have previously developed the VASH2-peptide vaccine as an antibody-based therapy targeting VASH2 (Lee et al. 2023). Because this treatment induced antibodies that worked from outside the cells, it did not alter the level of detyrosinated α-tubulin in the primary cancer (Supplementary Fig. S2). We have shown that this therapy is effective for the prevention of metastasis, but not tumor angiogenesis, in PDAC (Lee et al. 2023). Here, we evaluated the effect of the VASH2 peptide vaccine on $CD8^+$ cell infiltration into tumors. VASH2-peptide vaccine did not affect the infiltration of $CD8^+$ cells in primary or metastatic PDAC tumors (Fig. 8).

Discussion

We developed VASH2-targeting therapies for the treatment of various cancers, including VASH2-ASO as a nucleotide-based therapy (Horie et al. 2023) and a VASH2-peptide vaccine as an antibody-based therapy (Lee et al. 2023). Here, we evaluated the effects of those VASH2-targeting therapies on PDAC and demonstrated their efficacy in a mouse model.

VASH2-ASO blocks the synthesis of Vash2 protein. The immunostaining of detyrosinated α-tubulin revealed that intraperitoneal injection of naked VASH2-ASO exerted its knockdown effect on PDAC *in vivo*. Subsequently, we evaluated therapeutic efficacy. VASH2-ASO therapy slightly, but significantly, inhibited the growth of primary tumors in parallel with the inhibition of tumor angiogenesis and enhancement of vascular normalization. In addition, VASH2-ASO therapy prevented the accumulation of ascites and signs of peritoneal dissemination and inhibited distant metastasis to the liver and lungs. Moreover, VASH2-ASO therapy significantly increased $CD8^+$ cell infiltration, especially in metastatic tumors of the liver and lungs. Importantly, the effects caused by treatment with VASH2-ASO matched well with the KPC mouse model whose expression of *Vash2* was knocked down or knocked out (Iida-Norita et al. 2019).

VASH2-peptide vaccine induces antibodies that block the effects of VASH2 from outside cells. Indeed, VASH2-peptide vaccine did not affect intracellular detyrosinated α-tubulin in the primary cancer. Our previous study revealed that the VASH2-peptide vaccine was effective in inhibiting metastasis, but not angiogenesis, in PDAC (Lee

et al. 2023). This is probably because the domains of VASH2 for pro-metastasis and pro-angiogenesis are distinct, and antibodies induced by the VASH2-peptide vaccine preferentially recognize the domain for pro-metastasis (Lee et al. 2023). Nevertheless, as anti-angiogenic therapies exhibit little benefit in the treatment of pancreatic cancer (Craven et al. 2016; An et al. 2023), the lack of angiogenesis inhibition in the VASH2-peptide vaccine treatment may not be a weak point for the treatment of PDAC.

Accumulating evidence suggests that PDAC lacks immune effector cells, such as $CD8^+$ cells, within the tumor tissue, resulting in an immunosuppressive TME, which might be the major reason why immune checkpoint inhibitors are ineffective (Steele et al. 2016; Muller et al. 2022; Guo et al. 2023). We have shown that the deletion of *Vash2* gene recovers this abnormality, indicating that VASH2 is one of the principal factors that cause this immunosuppressive TME in PDAC (Iida-Norita et al. 2019). Here, we showed that VASH2-ASO therapy, but not VASH2-peptide vaccine therapy, increased $CD8^+$ cell infiltration, especially in metastatic tumors of the liver and lungs. These results suggest that the immunosuppressive TME of PDAC is caused by the intracellular activity of VASH2, and VASH2-targeting therapies, especially VASH2-ASO, may be a promising option for combination therapy with immune checkpoint inhibitors for PDAC. This concept is currently under investigation.

In view of the above results, we suggest differential application of these two therapies for the treatment of PDAC. VASH2-ASO therapy can be administered at any stage of PDAC. Normalization of tumor vasculature should enhance the effectiveness of combination therapies with not only immunotherapy but also chemotherapy and radiation therapy (Sato 2011; Yang et al. 2021). The inconvenience of this therapy is that the effect does not continue for a long time and requires repeated administration at an interval of 3-4 days. In contrast, the scope of application of the VASH2-peptide vaccine therapy may be limited. The best approach is to prevent metastasis and/or recurrence after successful initial surgical treatment. What is attractive about this therapy is that long-term effects can be expected by maintaining antibody titers with a booster.

Acknowledgments

This work was supported by a grant numbered 21 cm0106201h0006 from the Japan Agency for Medical Research and Development to Y.S. We thank Ms. Yuriko Fujinoya for technical assistance.

Conflict of Interest

The authors declare no conflict of interest.

References

Aillaud, C., Bosc, C., Peris, L., Bosson, A., Heemeryck, P., Van Dijk, J., Le Friec, J., Boulan, B., Vossier, F., Sanman, L.E., Syed, S., Amara, N., Coute, Y., Lafanechere, L., Denarier, E., et al. (2017) Vasohibins/SVBP are tubulin carboxypeptidases (TCPs) that regulate neuron differentiation. *Science*, **358**, 1448-1453.

An, Y.F., Pu, N., Jia, J.B., Wang, W.Q. & Liu, L. (2023) Therapeutic advances targeting tumor angiogenesis in pancreatic cancer: current dilemmas and future directions. *Biochim. Biophys. Acta Rev. Cancer*, **1878**, 188958.

Craven, K.E., Gore, J. & Korc, M. (2016) Overview of pre-clinical and clinical studies targeting angiogenesis in pancreatic ductal adenocarcinoma. *Cancer Lett.*, **381**, 201-210.

Guo, J., Wang, S. & Gao, Q. (2023) An integrated overview of the immunosuppression features in the tumor microenvironment of pancreatic cancer. *Front. Immunol.*, **14**, 1258538.

Gurreri, E., Genovese, G., Perelli, L., Agostini, A., Piro, G., Carbone, C. & Tortora, G. (2023) KRAS-dependency in pancreatic ductal adenocarcinoma: mechanisms of escaping in resistance to KRAS inhibitors and perspectives of therapy. *Int. J. Mol. Sci.*, **24**, 9313.

Halbrook, C.J., Lyssiotis, C.A., Pasca di Magliano, M. & Maitra, A. (2023) Pancreatic cancer: advances and challenges. *Cell*, **186**, 1729-1754.

Horie, S., Suzuki, Y., Yamamoto, T., Obika, S., Mohri, K., Kiyota, C., Ren, Q., Warashina, S., Wada, Y., Watanabe, Y., Mukai, H. & Sato, Y. (2023) Novel strategy of liver cancer treatment with modified antisense oligonucleotides targeting human vasohibin-2. *Cancer Sci.*, **114**, 3740-3749.

Iida-Norita, R., Kawamura, M., Suzuki, Y., Hamada, S., Masamune, A., Furukawa, T. & Sato, Y. (2019) Vasohibin-2 plays an essential role in metastasis of pancreatic ductal adenocarcinoma. *Cancer Sci.*, **110**, 2296-2308.

Khan, S., Budamagunta, V. & Zhou, D. (2023) Targeting KRAS in pancreatic cancer: emerging therapeutic strategies. *Adv. Cancer Res.*, **159**, 145-184.

Kim, J.C., Kim, K.T., Park, J.T., Kim, H.J., Sato, Y. & Kim, H.S. (2015) Expression of vasohibin-2 in pancreatic ductal adenocarcinoma promotes tumor progression and is associated with a poor clinical outcome. *Hepatogastroenterology*, **62**, 251-256.

Kitahara, S., Suzuki, Y., Morishima, M., Yoshii, A., Kikuta, S., Shimizu, K., Morikawa, S., Sato, Y. & Ezaki, T. (2014) Vasohibin-2 modulates tumor onset in the gastrointestinal tract by normalizing tumor angiogenesis. *Mol. Cancer*, **13**, 99.

Lee, E.S., Suzuki, Y., Tomioka, H., Nakagami, H. & Sato, Y. (2023) Development of a novel and simple anti-metastatic cancer treatment targeting vasohibin-2. *Tohoku J. Exp. Med.*, **261**, 239-247.

Muller, M., Haghnejad, V., Schaefer, M., Gauchotte, G., Caron, B., Peyrin-Biroulet, L., Bronowicki, J.P., Neuzillet, C. & Lopez, A. (2022) The immune landscape of human pancreatic ductal carcinoma: key players, clinical implications, and challenges. *Cancers* (*Basel*), **14**, 995.

Nieuwenhuis, J., Adamopoulos, A., Bleijerveld, O.B., Mazouzi, A., Stickel, E., Celie, P., Altelaar, M., Knipscheer, P., Perrakis, A., Blomen, V.A. & Brummelkamp, T.R. (2017) Vasohibins encode tubulin detyrosinating activity. *Science*, **358**, 1453-1456.

Norita, R., Suzuki, Y., Furutani, Y., Takahashi, K., Yoshimatsu, Y., Podyma-Inoue, K.A., Watabe, T. & Sato, Y. (2017) Vasohibin-2 is required for epithelial-mesenchymal transition of ovarian cancer cells by modulating transforming growth factor-beta signaling. *Cancer Sci.*, **108**, 419-426.

Salazar, J., Bracchiglione, J., Savall-Esteve, O., Antequera, A., Bottaro-Parra, D., Gutierrez-Valencia, M., Martinez-Peralta, S., Pericay, C., Tibau, A. & Bonfill, X.; Appropriateness of Systemic Oncological Treatments for Advanced Cancer (ASTAC) Research Group (2023) Treatment with anticancer drugs for advanced pancreatic cancer: a systematic review. *BMC Cancer*, **23**, 748.

Sato, Y. (2011) Persistent vascular normalization as an alternative

goal of anti-angiogenic cancer therapy. *Cancer Sci.*, **102**, 1253-1256.

Sato, Y. (2013) The vasohibin family: a novel family for angiogenesis regulation. *J. Biochem.*, **153**, 5-11.

Schepis, T., De Lucia, S.S., Pellegrino, A., Del Gaudio, A., Maresca, R., Coppola, G., Chiappetta, M.F., Gasbarrini, A., Franceschi, F., Candelli, M. & Nista, E.C. (2023) State-of-the-art and upcoming innovations in pancreatic cancer care: a step forward to precision medicine. *Cancers* (*Basel*), **15**, 3423.

Shibuya, T., Watanabe, K., Yamashita, H., Shimizu, K., Miyashita, H., Abe, M., Moriya, T., Ohta, H., Sonoda, H., Shimosegawa, T., Tabayashi, K. & Sato, Y. (2006) Isolation and characterization of vasohibin-2 as a homologue of VEGF-inducible endothelium-derived angiogenesis inhibitor vasohibin. *Arterioscler. Thromb. Vasc. Biol.*, **26**, 1051-1057.

Steele, C.W., Karim, S.A., Leach, J.D.G., Bailey, P., Upstill-Goddard, R., Rishi, L., Foth, M., Bryson, S., McDaid, K., Wilson, Z., Eberlein, C., Candido, J.B., Clarke, M., Nixon, C., Connelly, J., et al. (2016) CXCR2 inhibition profoundly suppresses metastases and augments immunotherapy in pancreatic ductal adenocarcinoma. *Cancer Cell*, **29**, 832-845.

Suzuki, Y., Kitahara, S., Suematsu, T., Oshima, M. & Sato, Y. (2017) Requisite role of vasohibin-2 in spontaneous gastric cancer formation and accumulation of cancer-associated fibroblasts. *Cancer Sci.*, **108**, 2342-2351.

Takahashi, Y., Koyanagi, T., Suzuki, Y., Saga, Y., Kanomata, N., Moriya, T., Suzuki, M. & Sato, Y. (2012) Vasohibin-2 expressed in human serous ovarian adenocarcinoma accelerates tumor growth by promoting angiogenesis. *Mol. Cancer Res.*, **10**, 1135-1146.

Tu, M., Li, H., Lv, N., Xi, C., Lu, Z., Wei, J., Chen, J., Guo, F., Jiang, K., Song, G., Gao, W. & Miao, Y. (2017) Vasohibin 2 reduces chemosensitivity to gemcitabine in pancreatic cancer cells via Jun proto-oncogene dependent transactivation of ribonucleotide reductase regulatory subunit M2. *Mol. Cancer*, **16**, 66.

Watanabe, K., Hasegawa, Y., Yamashita, H., Shimizu, K., Ding, Y., Abe, M., Ohta, H., Imagawa, K., Hojo, K., Maki, H., Sonoda, H. & Sato, Y. (2004) Vasohibin as an endothelium-derived negative feedback regulator of angiogenesis. *J. Clin. Invest.*, **114**, 898-907.

Xue, X., Gao, W., Sun, B., Xu, Y., Han, B., Wang, F., Zhang, Y., Sun, J., Wei, J., Lu, Z., Zhu, Y., Sato, Y., Sekido, Y., Miao, Y. & Kondo, Y. (2013) Vasohibin 2 is transcriptionally activated and promotes angiogenesis in hepatocellular carcinoma. *Oncogene*, **32**, 1724-1734.

Yang, T., Xiao, H., Liu, X., Wang, Z., Zhang, Q., Wei, N. & Guo, X. (2021) Vascular normalization: a new window opened for cancer therapies. *Front. Oncol.*, **11**, 719836.

Zhang, Y., Xue, X., Zhao, X., Qin, L., Shen, Y., Dou, H., Sun, J., Wang, T. & Yang, D.Q. (2018) Vasohibin 2 promotes malignant behaviors of pancreatic cancer cells by inducing epithelial-mesenchymal transition via Hedgehog signaling pathway. *Cancer Med.*, **7**, 5567-5576.

Supplementary Files

Please find supplementary file(s);
https://doi.org/10.1620/tjem.2023.J109